

RSC Advances



This is an *Accepted Manuscript*, which has been through the Royal Society of Chemistry peer review process and has been accepted for publication.

Accepted Manuscripts are published online shortly after acceptance, before technical editing, formatting and proof reading. Using this free service, authors can make their results available to the community, in citable form, before we publish the edited article. This *Accepted Manuscript* will be replaced by the edited, formatted and paginated article as soon as this is available.

You can find more information about *Accepted Manuscripts* in the [Information for Authors](#).

Please note that technical editing may introduce minor changes to the text and/or graphics, which may alter content. The journal's standard [Terms & Conditions](#) and the [Ethical guidelines](#) still apply. In no event shall the Royal Society of Chemistry be held responsible for any errors or omissions in this *Accepted Manuscript* or any consequences arising from the use of any information it contains.

ARTICLE

A new class of pyrenyl solid-state emitters: 1-pyrenyl ynones. Synthesis *via* the Friedel-Crafts route, molecular and electronic structure and photophysical properties†

Cite this: DOI: 10.1039/x0xx00000x

Received 00th January 2012,
Accepted 00th January 2012

DOI: 10.1039/x0xx00000x

www.rsc.org/Rafał Flamholz^a, Damian Plażuk^a, Janusz Zakrzewski^{a*}, Rémi Métivier^{b*}, Keitaro Nakatani^b, Anna Makal^c, Krzysztof Woźniak^c

Friedel-Crafts acylation of pyrene with alkynoic acids in the presence of trifluoroacetic anhydride and triflic acid constitutes a direct and efficient route to 1-pyrenyl ynones. These compounds in chloroform solutions emit fluorescence at longer wavelengths, with higher quantum yields and longer lifetimes than a typical saturated acylpyrene derivative, 1-acetylpyrene. Moreover, in contrast to 1-acetylpyrene, they are moderate solid-state emitters. Comparative DFT studies revealed strong stabilization of the LUMOs of 1-pyrenyl ynones in comparison to the LUMO of 1-acetylpyrene. The single-crystal X-ray structure of 1-(pyren-1-yl)but-2-yn-1-one showed π -interactions of pyrenyl moieties in the crystal lattice. Investigations of the solid-state fluorescence of this compound revealed emission from long-lived excited states, including excimer species.

Introduction

Pyrene and its derivatives have attracted considerable interest as materials for organic electronics,¹ fluorescent monomers,^{2,3} molecular probes,⁴⁻⁷ and sensors.^{8,9} Considerable effort has been focused on the development of synthetic routes to pyrenes bearing variable substituents^{1,10-12} and on studies of their fluorescence properties.^{13,14} Special attention has been paid to 1-pyrenyl carbonyl compounds such as aldehyde, ketones, acid, esters, amides, etc., exhibiting strongly environment-sensitive fluorescence and used as molecular probes.¹⁵⁻²¹ Recent works by the Konishi group have provided a basis for understanding the photophysical properties of this class of fluorophores.^{15-17,21} As far as pyrenyl ketones are concerned, research reports have mainly concentrated on pyrenyl alkyl ketones. This class of perylenyl fluorophores shows short fluorescence lifetimes (10^{-9} - 10^{-8} s, compared with $>10^{-7}$ s for pyrene) and low quantum yields due to efficient intersystem crossing.^{14,15} Only very recently have two reports appeared disclosing the synthesis and photophysical properties of the simplest pyrenyl alkynyl ketone, 1-propynylpyrene.^{22,23} This ketone offers a unique opportunity for attachment of a pyrene carbonyl tag to biomolecules or nanomaterials *via* azide-alkyne click chemistry.

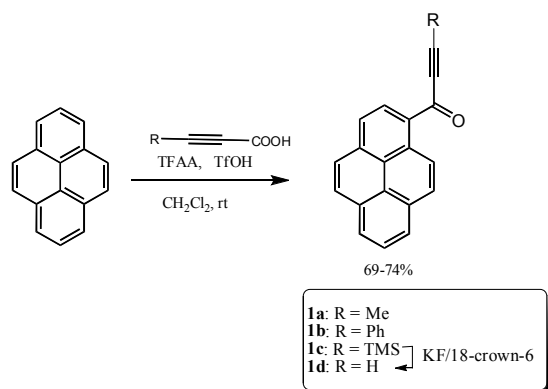
In a continuation of our research programme, which has focused on the use of functionalised carboxylic acids as acylating agents in Friedel-Crafts reaction, we recently elaborated an efficient method of synthesis of ferrocenyl ynones *via* a direct reaction of ferrocene with alkynoic acids in the presence of trifluoroacetic anhydride (TFAA) and trifluoromethanesulfonic acid (TfOH).²⁴ Herein we report that this approach may be used for simple and efficient synthesis of 1-pyrenyl ynones. We have also studied the fluorescence properties of these compounds which were compared to those of the simplest pyrenyl alkyl ketone, 1-acetylpyrene. Unexpectedly, we found that, in contrast to the latter compound, the synthesized 1-pyrenyl ynones display fluorescence not only in solution but also in the solid state. An X-ray diffraction study (including topological analysis of experimental charge density) performed for 1-(pyren-1-yl)but-2-yn-1-one revealed face-to-face π -stacking of the pyrene moieties in the crystal, thus suggesting that emission may originate from solid-state excimers. Finally, we carried out comparative DFT calculations on this compound and 1-acetylpyrene.

Results and Discussion

Synthesis of pyrenyl ynones 1a-d

Yrones or α,β -acetylenic ketones are versatile building blocks in organic synthesis, especially in the synthesis of heterocyclic compounds.²⁵ They can be synthesized via various routes starting from terminal alkynes.^{26,27,28,29} Readily available 2-alkynoic acids³⁰ are another potential starting material in ynone synthesis via Friedel-Crafts acylation of arenes. We reported the first example of such reaction, in which ferrocene was used as a reactive π -rich arene.²⁴ Since pyrene also exhibits high reactivity towards electrophiles, it seemed interesting to evaluate whether this approach can be used for a direct introduction of the alkynoyl group into this polycyclic arene.

The Friedel-Crafts reaction of pyrene with 2-alkynoic acids (Scheme 1) was carried out under conditions described earlier for ferrocene.²⁴ The isolated yields of compounds **1a-c** were in the range of 69–74%. Similarly, as in the case of ferrocene, the reaction of pyrene with propiolic acid (R=H) led to an intractable reaction mixture. However, compound **1d** was prepared in an almost quantitative yield (99%) by fluoride-promoted desilylation of **1c**.



Scheme 1. Synthesis of 1-pyrenyl yrones **1a-d**.

Structures of synthesized yrones **1a-d** were confirmed by spectroscopic and elemental analysis data (see ESI†). The simplest compound of this series, **1d**, was already reported in the literature. It was synthesised 40–44% overall in a reaction of pyrene-1-carboxaldehyde with ethynyl magnesium bromide²² (or TMS-ethynyl magnesium bromide followed by desilylation²³), and subsequent oxidation of the alcohol formed with Jones reagent. Compared to those methods our synthesis was simpler (using pyrene as the starting material) and more efficient (71% overall yield).

Molecular structure and crystal packing of **1a**

Crystals of **1a** that were suitable for X-ray diffraction study were obtained by slow diffusion of n-heptane into a solution of this compound in chloroform. Under these conditions **1a** crystallized in the centrosymmetric P2(1)/c space group in a monoclinic system, with one independent molecule in the crystallographic asymmetric

unit located in general position. The molecular structure of **1a** is presented in Fig. 1.

In the experimental structure of **1a** the pyrenyl moiety is not ideally planar, but slightly bent along its longer (C7 → C14) axis. The angle between the plane of ring C5, C6, C7, C8, C9, and C16 (ring 1) and that of ring C1, C2, C12, C13, C14, C15 (ring 2) is 3.7(3) degrees. The propynoyl substituent is twisted out of the

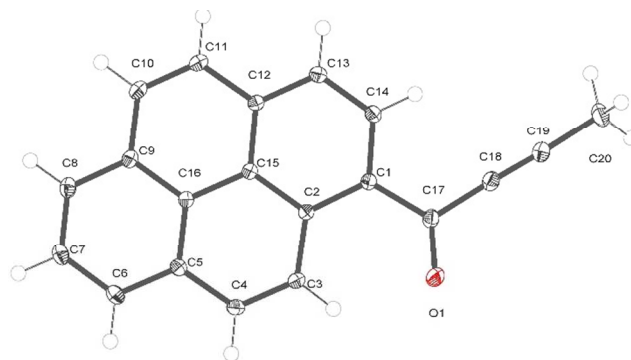


Fig. 1. ORTEP representation of **1a** with an atom numbering scheme. Atomic displacement parameters are drawn at 50% probability level.

plane of adjacent ring 2, as indicated by the C2-C1-C17-C18 and C14-C1-C17-O1 torsion angles which were significantly different from 180 degrees (172.37(7) degrees and C14 C1 C17 O1 168.68(9) degrees, respectively). The angle between the plane of ring 2 and the plane of the carbon yl moiety was 9.9(5) degrees. This conformation enables the formation of two weak intermolecular C-H...O hydrogen bonds in the crystal lattice: C4-H4...O1_i O1-H4 where the distance is 2.552(3) Å and C20-H20A...O1_{ii} O1-H20A where the distance is 2.579(3) Å (where *i* denotes the following symmetry transformation: 1-x, 2-y, 1-z and *ii* denotes the symmetry transformation: x, 1/2 - y, 1/2 + z) (Fig. 2).

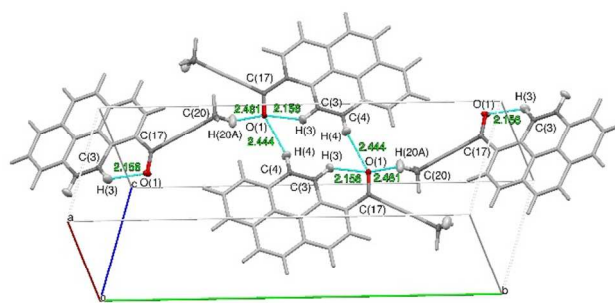


Fig. 2. C-H...O hydrogen bonds in a crystal structure of **1a**. The atoms involved in the hydrogen bonds are presented with thermal ellipsoids at 50%, the remaining atoms are represented in grey for clarity. The hydrogen bonds are highlighted in cyan. The H...A distances are reported in Å.

The tilt of the carbonyl group out of the ring 2 plane does not prevent the formation of a weak intramolecular C3-H3...O1 hydrogen bond, with an O1...H3 distance of only 2.156(1) Å. Viewed along the crystallographic [001] direction, the crystal packing of **1a** shows a characteristic herringbone motif (Fig. 3a) with distinct layers of molecules stacked along the [100] direction. Within the layers the carbonyl moieties are oriented almost parallel to the [001] direction; in consecutive layers the carbonyl groups point in opposite directions (i.e. the carbonyl moieties in one layer are almost parallel to [001] direction, while the carbonyl moieties from the next layer are almost antiparallel to this direction). The angle between the C17-O1 carbonyl bond and the crystallographic [001] direction is 25.8(5) degrees (for a molecule in the alternative layer this would be 205.8(5) degrees).

The crystal structure of **1a** can be considered as composed of layers of molecules with parallel dipole and transition moments; with the directions of these moments alternating between layers. Each layer can be further viewed as composed of strands of molecules, packed along the [001] direction.

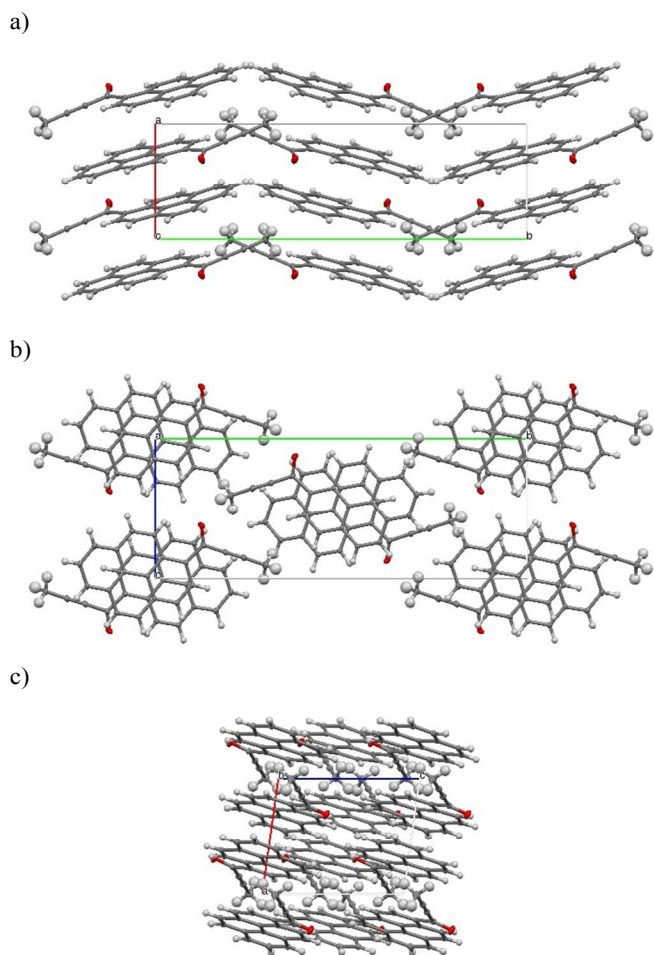


Fig. 3. Crystal packing of **1a**. (a) view along the [001] direction, (b) view along the [100] direction, (c) view along the

[010] direction. Crystal axes denoted as follows: a [100] as red, b [010] as green and c [001] as blue.

Molecules from consecutive layers along the [100] direction (Fig. 3b), related by crystallographic centres of inversion, are also involved in π -stacking interactions, thus building columns of symmetry-related molecules along [100] (Fig. 3a). Due to the 'bend' in the pyrene moiety, the closest contacts of an independent molecule (I) and the symmetry-related molecule II (above) are different from the closest contacts of an independent molecule (I) and the symmetry-related molecule III (below) (Fig. 4). For the former the closest contacts are C2_I – C12_II (3.377(3) Å) and C14_I – C16_II (3.419(3) Å), while for the latter the closest contacts are C1_I – C9_III (3.361(3) Å) and C15_I – C15_III (3.433(3) Å).

Interlayer interactions are stabilised by a weak C-H...O hydrogen bond: C4-H4...O1_i, while the separate layers are stabilised by a weak C-H...O hydrogen bond: C20-H20A...O1.

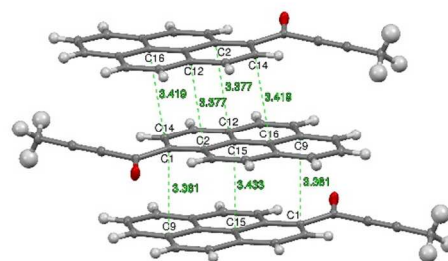


Fig. 4. Intermolecular contacts in layers of **1a** molecules along the [100] direction. The C...C distances are highlighted in green and reported in Å. Atomic displacement parameters are reported at 50% probability level.

Because the scattering power of the **1a** crystals was good, aspherical atomic scattering factors could be applied in structure refinement. Therefore, we could also perform a preliminary topological analysis of experimental charge density for this compound (see ESI[†]). It supports the structural analysis, thus confirming the presence and significance of all of the already mentioned C-H...O interactions. The strongest hydrogen bond that is present in the crystals of **1a** is the intramolecular C3 – H3 ... O1 bond, according to electron density and energy density criteria. A ring critical point was found within the C1-C2-C3- H3-O1-C17 ring, closed by this bond, thus confirming the significance of this interaction according to Koch and Popelier criteria.³¹ This analysis also demonstrated bond paths for the π -stacking interactions between symmetry-related molecules of **1a**, which may support the 'excimer' hypothesis (*vide infra*).

Table 1. The most important parameters of experimental charge density at bond critical points in **1a**. Symmetry operations: i: 1-x, 2-y, 1-z; ii: x, 1/2 - y, 1/2 + z; iii: -x, 2-y, -z; iv: 1-x, 2-y, -z.

The molecule of **1a** in the crystal is strongly polarized with a negative charge of over 0.5e localised on the butynoyl group and an equivalent positive charge residing on the pyrene moiety. This results in a significant molecular dipole moment, oriented in between the C1-C17 and C17-O1 bond axes and coplanar with the pyrene moiety. According to the DFT B3PW91 calculations, an isolated molecule of **1a** has the dipole moment of 3.8 D, while the dipole moment obtained from the experimental charge density model is almost 4 times larger (15.8 D). It must be stressed that the absolute value of the molecular dipole moment in the crystal cannot be reliably derived from the current experimental charge density model, and that the value only indicates a tendency for increased polarisation of the molecule in the crystalline environment. Quantum chemical calculations in the periodic lattice performed at the B3LYP level of theory with a 6-31+g(d) basis set yielded an optimised geometry that was identical to the geometry from X-ray diffraction within an experimental error. These calculations confirm enhancement of the molecular dipole moment in the crystal lattice. The resulting dipole moment has a direction that is in agreement with the results of experimental charge density analysis and the results of theoretical calculations for an isolated molecule and a value of 4.7 D. The dipole moment vector is almost perpendicular to the [100] crystallographic direction (~86 degrees) and coplanar with the pyrene moiety.

Photophysical properties of **1a-d** and **AcPyr** in solution.

The electronic absorption and emission spectra of **1a-d** and **AcPyr** in chloroform ($c=10^{-6}$ M) are shown in Fig. 5 and the spectral data are collected in Table 2. At such a low concentration the formation of aggregates and excimers is highly unlikely and the observed emission can be ascribed to fluorophore monomers.

The spectra reveal significant (up to ~60nm) bathochromic shifts of the bands of **1a-d** in comparison to those of **AcPyr**. This suggests that the alkynoyl substituents are more efficiently conjugated with the pyrenyl moiety than the acetyl group. Furthermore, the absorption bands of **1a-d** enter the visible region and these compounds can be excited with violet light. All of the investigated ketones are practically non-fluorescent in a nonpolar solvent, hexane (See ESI[†]). In a medium polarity solvent, chloroform, compounds **1a-d** showed fluorescence at 449-471 nm with quantum yields in the range of 0.02–0.07, whereas **AcPyr** emitted weakly at 409 nm (quantum yield was lower than 0.005). In a more polar aprotic solvent, DMSO, all **1a-d** were emissive, whereas in a polar but hydroxylic solvent, methanol, only **1a** was a strong emitter. Surprisingly, **1a-d** were stronger emitters in chloroform than in methanol, whereas the opposite effect was observed for **AcPyr**. Time-resolved fluorescence investigations of **1a-d** and **AcPyr** were performed in chloroform solutions and revealed multiexponential decays in all cases (Fig. 6a, Table 2). A fast decay was observed for **AcPyr**, intermediate behavior was observed for **1a** and **1c**, whereas much slower decays were

Interaction	$\rho(\text{r}_{\text{acr}})$ [e Å ⁻³]	Lap(r _{acr}) [e Å ⁴]	G(r _{acr}) [H a ₀ ⁻³]	V(r _{acr}) [H a ₀ ⁻³]	H(r _{acr}) [H a ₀ ⁻³]	G(r _{acr})/ [H e ⁻¹]	H(r _{acr})/ [H e ⁻¹]	V(r _{acr})/ G(r _{acr})
O1 ... H3	0.110(5)	2.076(4)	0.017	-0.013	0.004	1.043	0.245	0.765
H4 ... i_O1	0.056(5)	0.684(3)	0.006	-0.004	0.001	0.723	0.121	0.667
H20A ... ii_O1	0.045(4)	0.745(3)	0.006	-0.004	0.002	0.900	0.300	0.667
C2 ... iii_C12	0.031(1)	0.295(1)	0.002	-0.002	0.001	0.435	0.218	1.000
C14 ... iii_C16	0.029(1)	0.272(1)	0.002	-0.002	0.001	0.465	0.233	1.000
C1 ... iv_C9	0.036(2)	0.314(1)	0.003	-0.002	0.001	0.562	0.187	0.667
C15 ... iv_C15	0.021(2)	0.303(1)	0.002	-0.001	0.001	0.643	0.321	0.500

recorded for **1b** and **1d**. Three sets of decay time constants could be distinguished: a fast contribution ($\tau_1 < 0.15$ ns), an intermediate contribution ($\tau_2 = 0.2$ -0.3ns), and a slow contribution ($\tau_3 > 0.5$ ns).

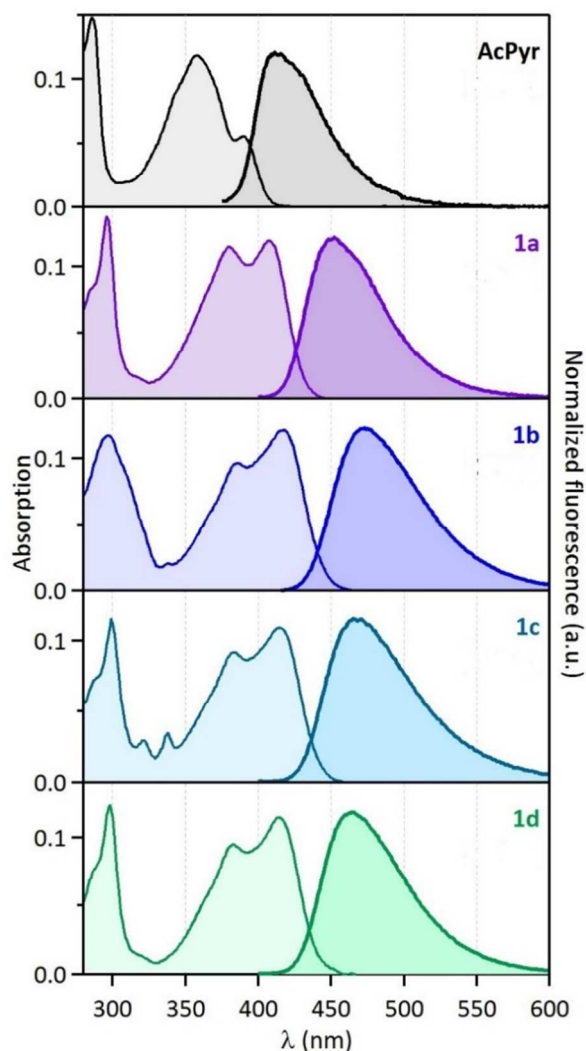


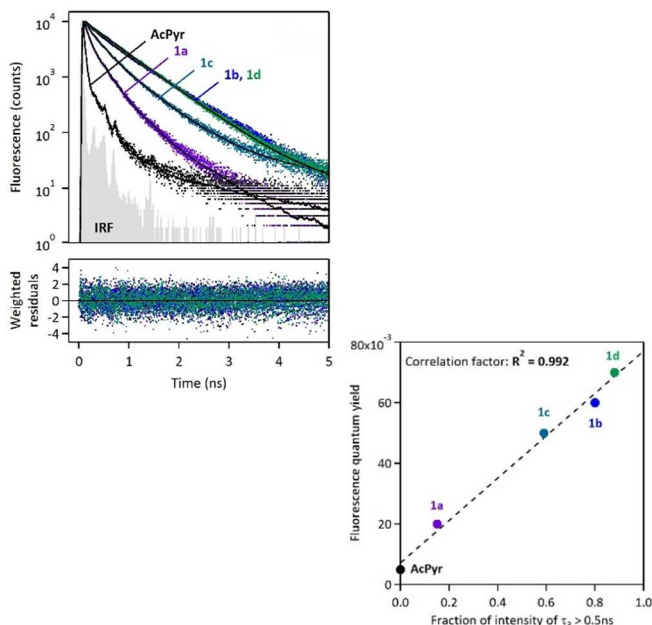
Fig. 5. Normalised absorption (left) and fluorescence (right) spectra of compounds **1a-d** and **AcPyr** in CHCl_3 ($\lambda_{\text{exc}} = 390$ nm for **1a-d** and 330nm for **AcPyr**).

These three contributions may be related to three populations of conformers having different relaxation times and different emission efficiencies. The fraction of intensity related to the

slowest component τ_3 is very much variable depending on the compound. It is absent for **AcPyr**, represents a small proportion for **1a** ($\phi_3 = 0.15$) and its contribution becomes predominant for compounds **1b** ($\phi_3 = 0.80$), **1c** ($\phi_3 = 0.59$), and **1d** ($\phi_3 = 0.88$). This fraction of intensity is well-correlated to the overall fluorescence quantum yields of compounds **AcPyr** and **1a-d** (Fig. 6b). Therefore, we could conclude that the slowest decay time corresponds to a conformer which is much more fluorescent than the others. Consequently, the fluorescence quantum yields measured in CHCl_3 reflect the various proportions of the different conformers, which are variable from one compound to another.

Table 2. Electronic absorption and fluorescence data for compounds **1a-d** and **AcPyr**.

	1a	1b	1c	1d	AcPyr
λ_{abs} (nm) (CHCl_3)	408	418	416	415	391
ϵ_{max} (M^{-1}cm) (CHCl_3)	15100	45500	18800	24800	15400
λ_{em} (nm) (CHCl_3)	449	471	462	460	409



Φ_F (CHCl_3)	0.02	0.06	0.05	0.07	<0.005
λ_{em} (nm) (solid)	569	530	550	565	486
Φ_F (solid)	0.13	0.04	0.12	0.07	-
τ_1 (ns) /contribution (CHCl_3)	0.11/0.67 0.29/0.29; 0.73/0.04	0.24/0.44; 0.77/0.56	0.20/0.65 0.60/0.35	0.24/0.25 0.68/0.75	0.06/0.89 0.27/0.11

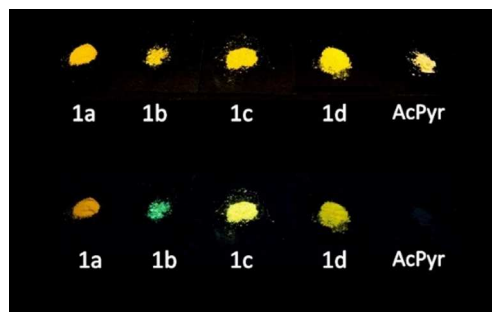


Fig. 6. (a) Fluorescence decay curves of **1a-d**

and **AcPyr** recorded in CHCl_3 , with multiexponential fitting and weighted residuals (IRF = instrumental response function). (b) Correlation plot between the fluorescence quantum yield measured in CHCl_3 and the fraction of intensity corresponding to the slowest contribution (typically with a decay time constant $> 0.5 \text{ ns}$).

Solid-state fluorescence of **1a-d**

In contrast to **AcPyr**, which is almost non-emissive in the solid state (it exhibits extremely weak fluorescence centred at 486 nm), ketones **1a-d** are moderate solid-state emitters (Fig. 7-8 and Table 2). The solid state fluorescence of these compounds is centred at 530-567 nm, i.e. $\sim 100 \text{ nm}$ red-shifted compared to solution emission. This large shift suggests that the emissive state may be rather different to that of the molecular monomer in solution. The fluorescence quantum yields are in the range of 0.04 (**1b**)–0.13 (**1a**). Compounds **1b** and **1d** did not show a noticeable increase in solid-state fluorescence quantum yields as compared to the CHCl_3 solution values, whereas **1a** showed a 6-fold and **1c** a 2.5-fold increase of the quantum yield. Moreover, solid-state excitation spectra were also very much red-shifted as compared to the CHCl_3 solution, with λ_{max} of the first band in the 430–470 nm range, corresponding to red-shift values from 20 nm (**1a**) up to 55 nm (**1d**).

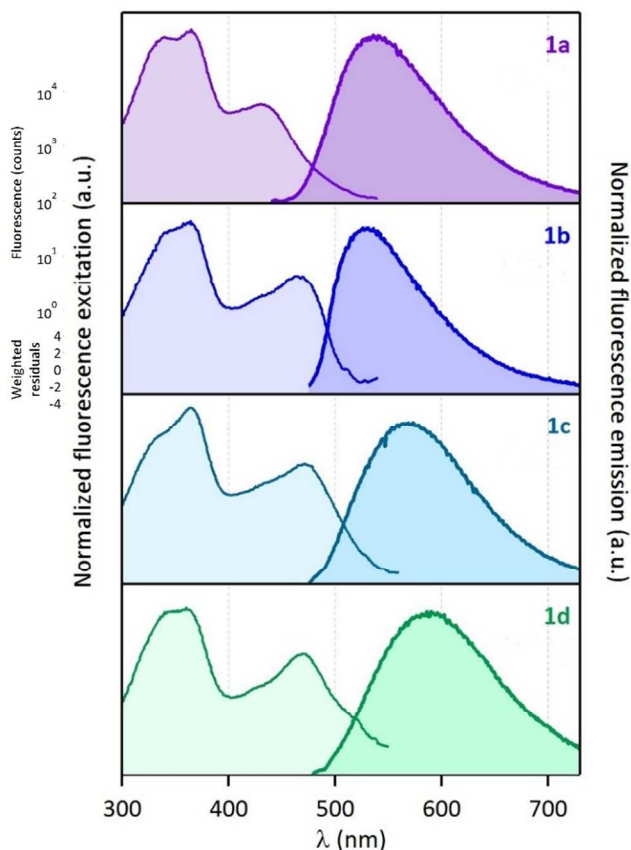
Fluorescence time-resolved experiments of **1a** were also performed in the solid state under ambient atmosphere. Fluorescence decay curves monitored at three different emission wavelengths ($\lambda_{\text{em}} = 540, 590$ and 640 nm) are shown in Fig. 9.

Fig. 7. Photographs of **1a-d** and **AcPyr** in the solid state under visible light (top row) and under 254 nm UV light (bottom row) illumination

Fig. 8. (Left) Normalized excitation and (right) emission spectra of compounds **1a-d** recorded in the solid state (powder inserted in an integration sphere). $\lambda_{\text{excit}} = 430\text{nm}$ for **1a** and 460nm for **1b-d**.

Global analysis was successfully applied to the three decays with multiexponential fitting and revealed three common components: two long decay times, $\tau_1 = 13.2\text{ ns}$ and $\tau_2 = 27.4\text{ ns}$ (which represented more than 99% of the fraction of intensity) and a short component, $\tau_3 \sim 0.6\text{-}1.2\text{ ns}$, which appeared either as

a decay time (for $\lambda_{\text{em}} = 540\text{ nm}$) or as a rise-time (for $\lambda_{\text{em}} = 590$ and 640 nm), as shown in Fig. 9. Such a short decay time in the blue-edge of the spectrum corresponding to a short rise-time in the red part of the spectrum is a typical signature of excimer formation which occurs within the crystal with a fast kinetic



rate. This mechanism is rather consistent with the face-to-face orientation of the pyrene moieties in the crystal lattice, as revealed by X-ray diffraction (*vide supra*).

It is generally believed that such an aggregation leads to non-emissive species (H-aggregates). However, some examples of emissive H-aggregates have been reported.³²⁻³⁴ In such aggregates, emission may arise from restriction of intramolecular rotation (RIR), blocking of nonradiative decay channels and from the formation of emissive solid-state excimers (meaning not only “excited dimers” but also “excited oligomers”). Consequently, **1a-d** emitted in the solid-state as monomers

(a green emission), but they also interacted very quickly in the excited state and led to strongly emissive excimer species (a red emission), and then following a very slow decay rate. This situation is different from the one observed in solution, where only fast monomer decays were observed.

Fig. 9. (a) Fluorescence decay curves of **1a** in the solid state, monitored at three different emission wavelengths ($\lambda_{\text{em}} = 540, 590$ and 640 nm), with multiexponential fitting and weighted residuals. (b) Zoomed region at short times, where excimer-type rise-time is clearly observed at $\lambda_{\text{em}} = 640\text{ nm}$, but absent at $\lambda_{\text{em}} = 540\text{ nm}$.

It should be emphasized that solid-state fluorescence, which is essential for various industrial applications, is still a relatively rare phenomenon because of the ubiquitous aggregation-caused quenching (ACQ) effect. Solid-state fluorophores exhibiting the aggregation-induced emission enhancement (AIEE) effect were discovered only very recently.³⁵⁻³⁷ Moreover, such fluorophores bearing a flat π -conjugated pyrene moiety are relatively rare.^{38,39,40} Strong yellow solid-state emission of **1a-d**, with long fluorescence decays, makes them promising candidates for the design of luminescent materials and devices.

Comparative DFT and TD DFT study of **1d** and **AcPyr**

To gain deeper insight into the influence of an acetylenic bond on the electronic structure of pyrene carbonyl chromophore DFT and TD DFT calculations were performed on the simplest ynone (**1d**) and **AcPyr**. It has to be mentioned that a DFT study of the latter molecule was recently published by Konishi et al.¹⁵ However, in the present work we focused our interest on a comparison of both compounds at the same calculation level. The B3PW91 functional with a 6-311+g(d) basis set was used since it provided satisfying results for structurally close alkynylferrocenes.⁴¹

are localized on the acyl groups, which results in a stronger (0.4 eV) stabilization of this orbital in **1d**. A significant difference in localization of electron density is observed for unoccupied LUMO, LUMO+1 and LUMO+2 orbitals. In the case of **AcPyr** these orbitals are localized on the pyrenyl moiety and the carbonyl group, whereas delocalization is observed on the ethynyl group in the case of **1d**. The strongest stabilization (~0.4-0.5 eV) is observed for the LUMO and LUMO+2 orbital of **1d**, in comparison to the same orbital in **AcPyr**.

We have also calculated the electronic absorption spectra of **1d** and **AcPyr** for isolated molecules and for a chloroform solution using time-dependent DFT and a polarizable continuum model (PCM) using integral equation formalism variant (IEFPCM). The data are gathered in Table 3.

Table 3. TD DFT-calculated electronic transitions in **1d** and **AcPyr**^a

a) Isolated molecules

Compound	λ_{\max}/nm (eV)	f	Main contribution(s)
1d	407.4 (3.04)	0.3985	H \rightarrow L (0.95)
	356.1 (3.48)	0.0527	H-1 \rightarrow L (0.79)
	292.1 (4.24)	0.1297	H \rightarrow L+1 (0.71)
	261.9 (4.73)	0.1231	H-4 \rightarrow L (0.79)
AcPyr	377.0 (3.29)	0.3523	H \rightarrow L (0.92)
	283.5 (4.37)	0.1909	H \rightarrow L+1 (0.45) H-1 \rightarrow L (0.19)
	247.6 (5.01)	0.1743	H-4 \rightarrow L (0.62)

b) CHCl₃ solution

Compound	λ_{\max}/nm (eV)	f	Main contribution(s)
1d	429.3 (2.89)	0.5538	H \rightarrow L (0.97)
	362.3 (3.42)	0.0774	H-1 \rightarrow L (0.85)
	296.4 (4.18)	0.2104	H \rightarrow L+1 (0.70)
	291.7 (4.25)	0.0510	H \rightarrow L+2 (0.73)
	266.9 (4.64)	0.1416	H-4 \rightarrow L (0.84)
	249.9 (4.96)	0.1003	H-5 \rightarrow L (0.89)
AcPyr	386.8 (3.21)	0.4962	H \rightarrow L (0.95)
	298.7 (4.15)	0.0525	H-3 \rightarrow L (0.64) H \rightarrow L+1 (0.22)
	287.0 (4.32)	0.2435	H \rightarrow L+1 (0.37) H-3 \rightarrow L (0.32)

The lowest energy band may practically be considered a pure HOMO-LUMO transition for both compounds. The calculated wavelengths of this band for the chloroform solution are in good agreement with the experimental values (429 vs. 415 nm for **1d** and 387 vs. 391 nm for **AcPyr**). It is generally believed that face-to-face H-aggregates are non-emissive in terms of Kasha's theory of exciton coupling. However, some examples of emissive H-aggregates have been reported.³²⁻³⁴ In such aggregates, emission may arise from restriction of intramolecular rotation (RIR), blocking nonradiative decay

channels or formation of emissive solid-state excimers (meaning not only "excited dimers" but also "excited oligomers"). A time-resolved fluorescence study clearly demonstrated that solid-state emission of **1a** originated from dynamic excimers formed during and shortly after the laser pulse and emitting at longer wavelengths than monomeric molecules. Some contribution from the RIR effect is also possible since the intermolecular hydrogen bond network along with π -stacking may severely inhibit rotational motions in individual fluorophores in the crystals.

Conclusions

We elaborated an efficient method of Friedel-Crafts acylation of pyrene with conjugated alkynoic acids which led to a new class of pyrenyl fluorophores – 1-pyrenyl ynones. Comparison of the electronic absorption and fluorescence emission spectra of these compounds with those of the simplest saturated pyrenyl ketone, 1-acetylpyrene, revealed some of their advantages. The lowest energy absorption bands of 1-pyrenyl ynones were shifted bathochromically to the visible region, therefore these compounds can be conveniently excited with violet light. They exhibit more intense fluorescence than 1-acetylpyrene in a medium polarity environment. Their fluorescence maxima are shifted towards lower energies by 50-60 nm and their fluorescence lifetimes are substantially longer than those of 1-acetylpyrene. In contrast to the latter compound, they exhibit strong fluorescence in the solid state, which is associated with long decay times and which can be attributed to an efficient formation of excimer species. Finally, the simplest ynone, 1-(pyren-1-yl)prop-2-yn-1-one, may be used in azide-alkyne click chemistry for introduction of a fluorescent pyrenyl tag to diverse molecular structures (biomolecules, polymers, etc.) This possibility is currently being studied in our laboratory and the results will be published in due time.

Acknowledgements

Financial support from the National Science Centre (Grant Harmonia UMO-2012/04/M/ST5/00712) is gratefully acknowledged. This research was also supported in part by the PL-Grid Infrastructure.

Notes and references

^a Department of Organic Chemistry, Faculty of Chemistry, University of Łódź, Tamka 12, 91-403 Łódź, Poland. E-mail: janjak@uni.lodz.pl

^b PPSM, ENS Cachan, CNRS, UniverSud, 61 av President Wilson, 94230 Cachan, France. E-mail: metivier@ppsm.ens-cachan.fr

^c Department of Chemistry, Warsaw University, Pasteura 1, 02-093 Warszawa, Poland

†Electronic Supplementary Information (ESI) available: Syntheses of **1a-d**. Electronic absorption and emission spectra of **1a-d** in various solvents. Details of X-ray diffraction and photophysical studies. See DOI: 10.1039/b000000x/

- 1 T. M. Figueira-Duarte and K. Müllen, *Chemical Reviews*, 2011, 111, 7260-7314.
- 2 F. Ciardelli, G. Ruggeri and A. Pucci, *Chemical Society Reviews*, 2013, 42, 857-870.
- 3 A. M. Breul, M. D. Hager and U. S. Schubert, *Chemical Society Reviews*, 2013, 42, 5366-5407.
- 4 G. Drummen, *Molecules*, 2012, 17, 14067-14090.
- 5 G. Bains, A. B. Patel and V. Narayanaswami, *Molecules*, 2011, 16, 7909-7935.
- 6 R. Métivier, I. Leray, M. Roy-Auberger, N. Zanier-Szydłowski and B. Valeur, *New Journal of Chemistry*, 2002, 26, 411-415.
- 7 R. Métivier, I. Leray, J.-P. Lefevre, M. Roy-Auberger, N. Zanier-Szydłowski and B. Valeur, *Physical Chemistry Chemical Physics*, 2003, 5, 758-766.
- 8 A. Bencini and V. Lippolis, *Coordination Chemistry Reviews*, 2012, 256, 149-169.
- 9 J. Xie, M. Ménand, S. Maisonneuve and R. Métivier, *The Journal of Organic Chemistry*, 2007, 72, 5980-5985.
- 10 L. Zöphel, V. Enkelmann and K. Müllen, *Organic Letters*, 2013, 15, 804-807.
- 11 X. Feng, J.-Y. Hu, F. Iwanaga, N. Seto, C. Redshaw, M. R. J. Elsegood and T. Yamato, *Organic Letters*, 2013, 15, 1318-1321.
- 12 Y. Niko, S. Kawauchi, S. Otsu, K. Tokumaru and G.-i. Konishi, *The Journal of Organic Chemistry*, 2013, 78, 3196-3207.
- 13 M. Ottonelli, M. Piccardo, D. Duce, S. Thea and G. Dellepiane, *Journal of Physical Chemistry A*, 2012, 116, 611-630.
- 14 C. X. Yao, H. B. Kraatz and R. P. Steer, *Photochemical & Photobiological Sciences*, 2005, 4, 191-199.
- 15 Y. Niko, Y. Hiroshige, S. Kawauchi and G.-i. Konishi, *Tetrahedron*, 2012, 68, 6177-6185.
- 16 Y. Niko, Y. Hiroshige, S. Kawauchi and G. I. Konishi, *Journal of Organic Chemistry*, 2012, 77, 3986-3996.
- 17 Y. Niko, S. Kawauchi and G. I. Konishi, *Tetrahedron Letters*, 2011, 52, 4843-4847.
- 18 A. Jana, S. Atta, S. K. Sarkar and N. D. P. Singh, *Tetrahedron*, 2010, 66, 9798-9807.
- 19 K. Szczubiałka, Ł. Moczek, A. Goliszek, M. Nowakowska, A. Kotzev and A. Laschewsky, *Journal of Fluorine Chemistry*, 2005, 126, 1409-1418.
- 20 L. Bucsiöva, P. Hrdlovič and Š. Chmela, *Journal of Photochemistry and Photobiology a-Chemistry*, 2001, 143, 59-68.
- 21 Y. Niko and G.-i. Konishi, *Journal of Synthetic Organic Chemistry Japan*, 2012, 70, 918-927.
- 22 D. A. Fleming, C. J. Thode and M. E. Williams, *Chemistry of Materials*, 2006, 18, 2327-2334.
- 23 S. P. Sau and P. J. Hrdlicka, *The Journal of Organic Chemistry*, 2011, 77, 5-16.
- 24 D. Plažuk and J. Zakrzewski, *Journal of Organometallic Chemistry*, 2009, 694, 1802-1806.
- 25 B. Willy, T. J. J. Müller, *Arkivoc* 2008 (i) 195-208.
- 26 M. Navidi, B. Movassagh, *Monatsh. Chem.* 2013, 144, 1363-1367.
- 27 W. Sun, Y. Wang, X. Wu and X. Yao, *Green Chemistry*, 2013, 15, 2356-2360.
- 28 B. Huang, L. Yin and M. Cai, *New Journal of Chemistry*, 2013, 37, 3137-3144.
- 29 M. Navidi, B. Movassagh and S. Rayati, *Applied Catalysis A: General*, 2013, 452, 24-28.
- 30 N. M. Carballeira, *Chemistry and Physics of Lipids*, 2013, 172-173, 58-66.
- 31 U. Koch and P. L. A. Popelier, *The Journal of Physical Chemistry*, 1995, 99, 9747-9754.
- 32 V. Karunakaran, D. D. Prabhu and S. Das, *The Journal of Physical Chemistry C*, 2013, 117, 9404-9415.
- 33 U. Rösch, S. Yao, R. Wortmann and F. Würthner, *Angewandte Chemie International Edition*, 2006, 45, 7026-7030.
- 34 S. Varghese and S. Das, *The Journal of Physical Chemistry Letters*, 2011, 2, 863-873.
- 35 S. P. Anthony, *ChemPlusChem*, 2012, 77, 518-531.
- 36 M. Shimizu and T. Hiyama, *Chemistry - An Asian Journal*, 2010, 5, 1516-1531.
- 37 Y. Hong, J. W. Y. Lam and B. Z. Tang, *Chemical Communications*, 2009, 4332-4353.
- 38 Q. Feng, M. Wang, B. Dong, C. Xu, J. Zhao and H. Zhang, *CrystEngComm*, 2013, 15, 3623-3629.
- 39 P. Kotchapradist, N. Prachumrak, R. Tarsang, S. Junguttiwong, T. Keawin, T. Sudyoadsuk and V. Promarak, *Journal of Materials Chemistry C*, 2013, 1, 4916-4924.
- 40 Y. Li, D. Wang, L. Wang, Z. Li, Q. Cui, H. Zhang and H. Yang, *Journal of Luminescence*, 2012, 132, 1010-1014.
- 41 D. Plažuk, J. Zakrzewski, K. Nakatani, A. Makal, K. Woźniak and S. Domagala, *Rsc Advances*, 2012, 2, 3512-3524.